CASE REPORT

Annals of Agricultural and Environmental Medicine
www.aaem.pl

Meningoencephalitis and postinflammatory hydrocephalus in the course of COVID-19 disease in newborn – the potential role of acetazolamide as add-on therapy to the standard treatment

Sławomir Jan Wątroba[1,A,E-F], **Jarosław Bryda**[2,B-D]

[1] *Department of Neonatology and Neonatal Intensive Care Unit, Independent Public Healthcare, Puławy, Poland*
[2] *Department of Veterinary Hygiene, Voivodship Veterinary Inspectorate, Lublin, Poland*
A – Research concept and design, B – Collection and/or assembly of data, C – Data analysis and interpretation, D – Writing the article, E – Critical revision of the article, F – Final approval of the article

Wątroba SJ, Bryda J. Meningoencephalitis and postinflammatory hydrocephalus in the course of COVID-19 disease in newborn – the potential role of acetazolamide as add-on therapy to the standard treatment. Ann Agric Environ Med. doi: 10.26444/aaem/154827

Abstract

The topic of SARS-CoV-2 coronavirus infections in children is still complex and not fully understood. Acute meningoencephalitis (ME) was not considered a common presentation of COVID-19 in paediatrics, however, over time, several paediatric patients with ME associated with SARS-CoV-2 coronavirus infection have been described. The case report describes the clinical case of a newborn admitted to the Neonatal Intensive Care Unit (NICU) on 11th day of life due to severe SARS-CoV-2 coronavirus infection, who experienced multiple seizure episodes. The patient was diagnosed with ME and hydrocephalus. In the absence of clinical improvement, despite the use of standard treatment, acetazolamide (ACZ) was used, achieving complete relief of seizures and gradual regression of hydrocephalus. This means that ACZ can be considered as an add-on therapy to standard treatment in cases of ME and postinflammatory hydrocephalus in the course of COVID-19 disease.

Key words

newborn, meningoencephalitis, COVID-19, hydrocephalus, acetazolamide, environmental microbiology

Abbreviations

ABB – acid-base balance; **ACV** – aciclovir; **ACZ** – acetazolamide; **ALP –** alkaline phosphatase; **AMP –** ampicillin; **ARDS –** acute respiratory distress syndrome; **CA** – carbonate dehydratase; **CMV –** cytomagalovirus; **CNS –** central nervous system; **CPE –** carbapenamase-producing Enterobacteriaceae; **CSF –** cerebrospinal fluid; **CTX –** cefotaxime; **ECG –** electrocardiogram; **EEG –** electroencephalogram; **FFP –** fresh frozen plasma; **FiO_2 –** oxygen concentration in the breathing mixture; **FLC –** fluconazole; **FR –** ferritin; **GBS –** group B Streptococcus; **GM –** gentamicin; **HFNC –** high-flow nasal cannula; **IVH –** intraventricular haemorrhage; **LP** – lumbar puncture; **ME –** meningoencephalitis; **MP –** meropenem; **MRI –** magnetic resonance imaging; **MRSA –** methicillin-resistant Staphylococcus aureus; **MSSA –** methicillin-sensitive Staphylococcus aureus; **NICU –** neonatal intensive care unit; **PB –** phenobarbital; **PC** – platelet concentrate; **PIMS** – paediatric inflammatory multisystem syndrome; **PVH –** periventricular haemorrhage; **RAV –** right axillary vein; **RSV –** respiratory syncytial virus; **RT-PCR –** real-time reverse transcription polymerase chain reaction; **SI –** singal intensity; **TnT –** troponin T; **USG** – ultrasonography; **VAN –** vancomycin

INTRODUCTION

The case study presents the analysis of a clinical case of a neonate with meningoencephalitis (ME) and postinflammatory hydrocephalus in the course of COVID-19 disease. Additionally, when preparing this manuscript, a review was undertaken of the available data in 2,540 publications on the epidemiology of SARS-CoV-2 coronavirus infections in newborns and children, with particular emphasis on the neurological complications of infections and the principles of their treatment. The potential role of carbonate dehydratase (CA) inhibitor – acetazolamide (ACZ) in inhibiting the progression of postinflammatory hydrocephalus in the course of COVID-19 disease was indicated.

✉ Address for correspondence: Sławomir Jan Wątroba, Department of Neonatology and Neonatal Intensive Care Unit, Independent Public Healthcare, Bema 1, 24-100 Puławy, Poland
E-mail: watrobaslaw@gmail.com

Received: 25.05.2022; accepted: 21.09.2022; first published: 28.09.2022

CASE REPORT

The subject of this report is a male newborn, born naturally in a provincial hospitals in the 39th week of pregnancy, in good general condition. The Apgar score: 1 minute – 10 points, 5 minutes – 10 points. Maternal pregnancy was complicated by urinary tract infection. Screening the mother for Group B Streptococcus (GBS) was negative. After birth, the newborn received antibiotic therapy with ampicillin (AMP) and gentamicin (GM) followed by standard doses of meropenem (MP) due to pneumonia, thrombocytopenia and intrauterine infection, which developed shortly after giving birth. Due to thromboctyopenia 50,000 cells/µl, the treatment included etamsylate, human immunoglobulins and fresh frozen plasma (FFP) – AB group. On the 9th day of life, the child was diagnosed with 3 episodes of tonic-clonic convulsions and phenobarbital (PB) was included in the treatment on a regular schedule of 20 mg i.v. every 8 hours. It is not clear why, apart from the standard

empirical treatment with the use of AMP and GM, MP was included in the treatment because the first blood culture was negative. It is not clear why thrombocytopenia was treated with FFP and not a plateled concentrate (PC), and why human immunoglobulins were used without confirmation of the immune etiology of thrombocytopenia. Despite the convulsions observed in the newborn, lumbar puncture (LP) was not performed. LP is contraindicated in a patient with thrombocytopenia; however, LP was also not performed after resolution of thrombocytopenia. After the first episode of seizures, ultrasound (USG) diagnosis of the central nervous system (CNS) was performed in the newborn, which showed increased echogenicity and features of thickening of the soft dura and arachnoid, increased furrows echogenicity, slight blurring of the boundaries between bends and furrows, increased echogenicity of the periventricular white matter, thickened outlines of the walls of the ventricular system, irregular outlines of choroid plexuses and features of hydrocephalus with an Evans index of 0.31. Only a study description was delivered. No printouts from the videoprinter were delivered.

On 11th day of life, a positive RT-PCR test of nasopharyngeal swab for SARS-CoV-2 coronavirus infection was obtained from the newborn. As a matter of urgency, the newborn was transferred to the Department of Neonatology and Neonatal Intensive Care Unit (NICU), that specializes in treating COVID-19 in newborns, for further diagnosis and specialist treatment.

On admission to the NICU of Independent Public Healthcare in Puławy, the neonate was in a mediocre condition, with clinical signs of sepsis, pale coats of a grey shade, delayed capillary relief time (4–6 seconds), increased muscle tone, crying with a high acoustic tone, fontanel tight non-pulsating, wide cranial sutures, fever up to 39°C, no jaundice. Another nasopharyngeal swab was taken for RT-PCR testing for SARS-CoV-2 coronavirus infection, which obtained a positive result, and the diagnostic and treatment procedures were continued according to the epidemiological standards in force.

The newborn was placed in an incubator closed in an isolation room with air underpressure relative to the surroundings and continuous monitoring of vital signs was applied. Due to numerous desaturations, non-invasive respiratory support in the form of high flow nasal cannula (HFNC) with the concentration of oxygen in the respiratory mixture (FiO2) equal to 30% was included in the treatment.

Table 1. Examination of cerebrospinal fluid (CSF)

Parameter	Test result	Reference range
Colour	bright red	-
Colour after centrifuging	water clear	-
Protein [mg/dl]	102.0	15.0 – 130.0
Chlorides [mmol/l]	121.3	115.0 – 130.0
Cytosis [cells/µl]	144	0 – 3
Glucose [mg/dl]	58.0	40.0 – 70.0
Volume [ml]	3.0	-
Limphocytes [%]	87.5	-
Clarity	slightly cloudy	-
Clarity after centrifuging	Incomplete	-
Segmental neutrocytes [%]	12.5	-

Acid-base balance (ABB) parameters were systematically monitored. Material was collected for bacteriological and laboratory tests. Influenza virus type A and B and respiratory syncytial virus (RSV) infection were excluded. LP was performed without complications, CSF was collected for general examination, microbiological examination and molecular examination. Chest X-ray diagnostics showed the presence of inflammatory lesions in the lungs. The central vessels were cannulated through the right axillary vein. In the treatment, fluconazole (FLC) at a daily dose of 10 mg/kg b.w. administered every 24 hours, acyclovir (ACV) at a daily dose of 30 mg/kg b.w. administered in 3 divided doses, cefotaxime (CTX) at a daily dose of 200 mg/kg b.w. administered in 4 divided doses, MP in a daily dose of 120 mg/kg b.w. administered in 3 divided doses and vancomycin (VAN) at a daily dose of 30 mg/kg b.w. given in 3 divided doses. Additionally, analgesic and antipyretic treatment and intravenous fluid therapy was applied. Despite the absence of clinically symptomatic seizures, anticonvulsant therapy with PB was maintained with gradual dose reduction until complete discontinuation. A blood culture mi\crobiological study showed an increase in methicillin-sensitive Staphylococcus aureus (MSSA). Blood was collected for the control culture. Inflammatory CSF with lymphocyte-predominant pleocytosis (Tab. 1). CSF culture was negative. Molecular diagnosis of CSF towards aerobic and enveloped bacteria negative (Tab. 2). Serological diagnosis for toxoplasmosis was negative. Molecular diagnostics of urine and CSF for cytomegalovirus (CMV) infection using the RT-PCR method were negative. RT-PCR diagnosis of the cerebrospinal fluid (CSF) for SARS-CoV-2 coronavirus infection was negative. Nasal smear culture for methicillin-resistant Staphylococcus aureus (MRSA) was negative. Rectal swab culture for carbapenamase-producing Enterobacteriaceae (CPE) was negative. Laboratory tests (Tab. 3) revealed an increased concentration of inflammatory markers, including ferritin (FR), moderate signs of anaemia and increased of alkaline phosphatase (ALP) activity. The concentration of thyroid hormones was normal. Biochemical markers of liver and kidney function were normal. Coagulation parameters were in the standard typical for age. Activity of biochemical markers of myocardial damage was typical for age. The result of the general urine test was normal. Markers of hepatic cholestasis was negative. In the electrocardiogram (ECG), the sinus rhythm, regular, without arrhythmias and without changes in the ST-T section. Diuresis and blood pressure were normal. On the basis of USG of the abdominal cavity, the presence of a gallbladder pseudopolyp was found, most likely in the course of the concentrated bile syndrome, and a slight enlargement of the calicael-pelvic system in the right kidney.

Table 2. RT-PCR diagnostics of cerebrospinal fluid (CSF) for aerobic and enveloped bacteria

Microorganism	Test result
Neisseria meningitidis	no DNA detected
Streptococcus pneumoniae	no DNA detected
Haemophillus influenzae	no DNA detected
Streptococcus agalactiae	no DNA detected
Escherichia coli	no DNA detected
Listeria monocytogenes	no DNA detected

Table 3. Results of selected biochemical blood tests.

Parameter	Reference range	Test result – 11th day of life	Test result – 15th day of life	Test result – 20th day of life
Albumin [g/dl]	3.50 – 5.20	3.40	3.30	-
ALT [U/l]	0.0 – 50.0	34.0	41.0	32.0
AST [U/l]	0.0 – 50.0	44.0	50.0	37.0
Total protein [g/dl]	4.1 – 6.3	5.7	-	-
CRP [mg/l]	0.0 – 5.0	13.0	5.0	1.0
Total bilirubin [mg/dl]	0.30 – 1.20	0.46	-	-
Chlorides [mmol/l]	101.0 – 109.0	102.0	-	-
CK-MB mass [ng/ml]	0.10 – 4.87	2.18	4.43	4.05
Ferritin [ng/ml]	30.0 – 400.0	551.0	-	572
Fibrynogen [mg/dl]	200.0 – 393.0	158.0	570.0	-
ALP [U/l]	43.0 – 115.0	93.0	-	-
FT 4 [pmol/l]	11.5 – 28.3	16.1	14.6	-
Glucose [mg/dl]	40.0 – 145.0	86.0	81.0	81.0
CK [U/l]	0.0 – 171.0	44.0	66.0	-
LDH [U/l]	108.0 – 430.0	451.0	276.0	-
Magnesium [mmol/l]	0.73 – 1.06	0.73	0.73	0.75
Urea [mg/dl]	8.0 – 26.0	39.0	22.0	-
NT-proBNP [pg/ml]	0.0– 7250.0	1235.0	362.0	919.0
PCT [ng/ml]	<0,5	0.06	0.08	0.02
Sodium [mmol/l]	136.0 – 146.0	138.0	137.0	-
Triglycerydes [mg/dl]	0.0 – 150.0	160.0	-	-
Troponin T hs [ng/ml]	0.000 – 0.100	0.059	0.116	0.058
TSH [µlU/ml]	0.72 – 11.00	1.21	3.63	-
Calcium [mmol/l]	2.25 – 2.75	2.38	2.59	2.76
APTT [seconds]	25.4 – 36.9	22.0	25.9	-
INR	0.8 – 1.2	0.87	0.86	-
Prothrombin time [seconds]	9.4 – 12.5	10.1	10.0	-
Prothrombin index [%]	80.0 – 120.0	129.0	131.0	-
Creatinine [mg/dl]	0.67 – 1.17	0.28	0.19	0.14
Thrombocytes [K/µl]	160.0 – 380.0	260.0	657.0	517.0
WBC [K/µl]	5.00 – 21.00	15.17	14.30	11.47
HCT [%]	39.0 – 50.0	45.5	34.3	29.3
HGB [g/dl]	10.0 – 18.0	16.2	12.2	11.7
RBC [M/µl]	3.80 – 6.00	4.62	3.53	3.10

ALT – alanine aminotransferase; **AST** – asparaginian aminotransferase; **ALP** – alkaline phosphatase; **APTT** – activated partial thromboplastin time; **CRP** – C-reactive protein; **CK** – creatine kinase; **CK-MB** – cardiac isoenzyme of creatine kinase; **FT4** – thyroxine; **HCT** – hematocrit; **HGB** – haemoglobin; **INR** – international normalised ratio; **NT-proBNP** – amino-terminal pro-brain natriuretic peptide; **LDH** – lactate dehydrogenase; **WBC** – white blood cells

On 14th day of life, USG of the CNS was performed, which showed increased echogenicity and features of thickening of the soft dura and arachnoid, increased furrows echogenicity, slight blurring of the boundaries between bends and furrows, increased echogenicity of the periventricular white matter, thickened outlines of the walls of the ventricular system, irregular outlines of choroid plexuses (Fig. 1), and no ventricular dilation with Evans index of 0.28 (Fig. 2).

On 19th day of life, a control USG of the CNS was performed, which showed postinflammatory hydrocephalus with an increase in the Evans index value from 0.28 to 0.38, without signs of intraventricular haemorrhage (IVH) or periventricular haemorrhage (PVH) (Fig. 3). Due to the features of hydrocephalus and convulsions, ACZ was included in the treatment at a dose of 15 mg/kg b.w. per day and antibiotic therapy was continued for another 3 weeks, until the control blood culture was negative and the patient's clinical condition was fully normalized, as well as normalization of the results of additional tests and vital signs, and regression of inflammatory changes on the control chest X-ray. In the control USG examinations of the CNS, a gradual regression of hydrocephalus was observed with a final reduction of the Evans index from 0.38 to 0.31 (Fig. 4). Acute, full-symptomatic inflammation of the lacrimal sac of the left eye was observed. The treatment included mechanical cleansing procedures, local sympathomimetics, as well as antibiotic therapy and local steroid therapy, which resulted in complete resolution of inflammation and restoration of normal eyeball mobility (Fig. 5).

After 10 days of hospitalization, a control nasopharyngeal swab for RT-PCR testing for SARS-CoV-2 coronavirus infection was made; the result was negative.

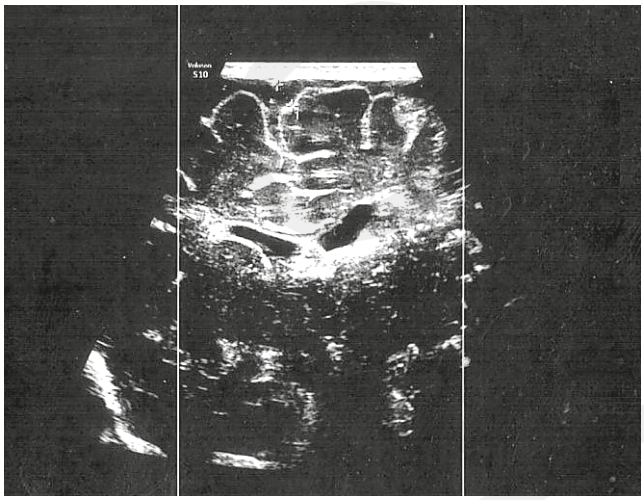

Figure 1. Central nervous system ultrasonography -14th day of life. Increased echogenicity and features of thickening of soft dura and arachnoid, increased furrows echogenicity, slight blurring of boundaries between bends and furrows. Low quality photo – scan of videoprinter printout

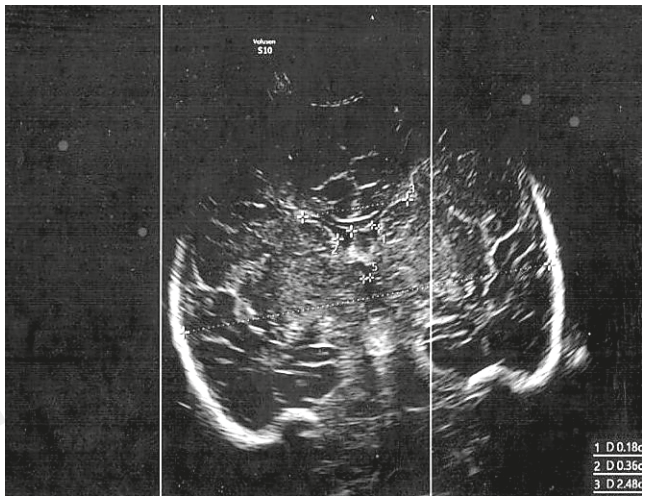

Figure 2. Central nervous system ultrasonography -14th day of life. Brain tissues without obvious focal lesions. Midline, interhemispheric not displaced. Asymmetry of the ventricular system of the brain in terms of the lateral ventricles. The anterior horns of the lateral ventricles in the frontal section with dimensions on the right side – 0.36 cm, on the left side – 0.18 cm. The posterior horns of the lateral ventricles in a sagittal cross-section with dimensions on the right side – 1.11 cm, on the left side -0.92 cm. Spread of the anterior horns of lateral ventricles – 2.48 cm, greatest width of the skull – 8.73 cm. Evans index – 0.28. Third ventricle of correct width – 0.15 cm. Choroidal plexuses symmetrical, homogeneous, without ultrasound features of IVH. Increased fluid around the choroidal plexuses. Increased echogenicity of the periventricular white matter. Fourth ventricle without features of expansion. Subdural space not extended – 0.14 cm wide. Structures of the posterior cranial fossa – no signs of pathology found. Low quality photo – a scan of the videoprinter printout

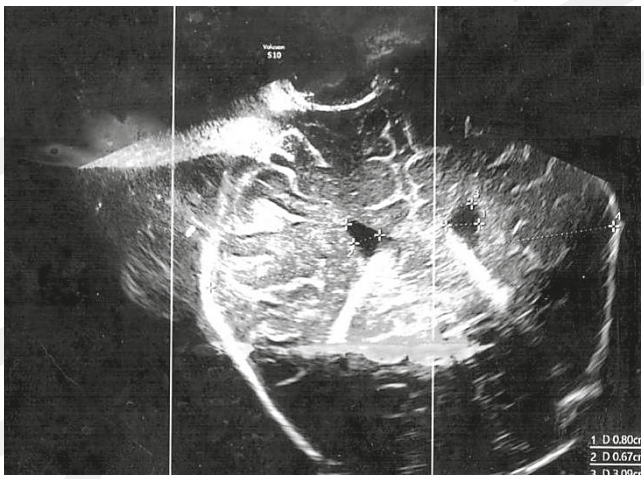

Figure 3. Central nervous system ultrasonography – 19th day of life. Brain without obvious focal changes. Irregular interhemispheric midline, not displaced. The anterior horns of the lateral ventricles in the frontal section with dimensions – on the right side – 0.67 cm, on the left side – 0.80 cm. The posterior horns of the lateral ventricles in a sagittal cross-section with dimensions – on the right side – 1.52 cm, on the left side -1.41 cm. The spread of the anterior horns of the lateral ventricles -3.09 cm, with the greatest width of the skull equal to 8,1 cm. Evans index – 0.38. Third ventricle with a width of 0.27 cm. Choroidal plexuses symmetrical, homogeneous, without ultrasound features of IVH. Increased fluidaround the choroidal plexuses. Discreetly increased periventricular echogenicity of white matter. Fourth ventricle in the frontal section with a width of 0.21 cm. The subdural spacenon dilated -0.32 cm. In the structures of the posterior cranial fossa, no signs of pathology were found. Low quality photo – a scan of the printout from the videoprinter

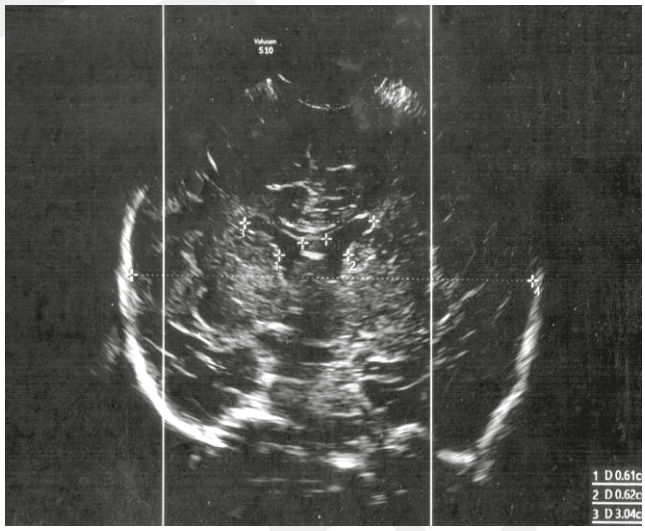

Figure 4. Central nervous system ultrasonography – 33th day of life. Brain tissues without obvious focal lesions. Irregular interhemispheric midline, not displaced. The anterior horns of the lateral ventricles in the frontal section with dimensions – on the right side – 0,61 cm, on the left side – 0,62 cm. The posterior horns of the lateral ventricles in a sagittal cross-section with dimensions -on the right side – 1.41 cm, on the left side – 1.30 cm. The spread of the anterior horns of the lateral ventricles – 3.04 cm, with the greatest width of the skull equal to 9.61 cm. Evans index incorrect – 0.31. Third ventricle – 0.27 cm. Choroidal plexuses symmetrical, homogeneous, without ultrasound features of IVH. Visibly increased fluid around the choroidal plexuses. Increased echogenicity of the periventricular white matter. In the structures of the posterior cranial fossa, no signs of pathology were found. Low quality photo – a scan of the printout from the videoprinter

The newborn was discharged home on the 35th day of life in good general condition, with no clinical signs of infection, with a normal pulse in the brachial and femoral arteries, normal saturation measurement, without abnormal neurological symptoms and normal muscle tone. The newborn was normally active, eagerly sucking, with normal gain in body weight, and was referred for routine cardiological diagnostics. An echocardiographic examination was performed in which no abnormalities were found, and the cardiological features of paediatric multisystemic inflammatory syndrome (PIMS) with a clinically silent course were excluded.

The newborn was consulted neurologically. Following the recommendation of the neurologist, magnetic resonance imaging (MRI) of the CNS was scheduled to be performed 4 weeks after the newborn's discharge fromhospital. On the 71th day of life, MRI of the CNS was performed, which in thin-film sections showed the presence of areas of increased signal intensity (SI) subcortex in the right frontal lobe, visible only in AX FLAIR MPR sections, most likely corresponding

Figure 5. Acute inflammation of the lacrimal sac

to the cortical system, on both sides, in the frontal parietal area, non-specific foci with elevated IS visible and most likely corresponding to post-inflammatory changes and dilatation the lateral ventricles of the brain without features of displacement with the Evans index 0.31 (Fig. 6). No pathological waves were found in electroencephalography (EEG) (Fig. 7). The newborn was left under the care of a neurologist and referred to a physiotherapist.

Rehabilitation with the NDT Bobath method was started with good results, and the psychophysical development of the infant at 6 months of age was defined as normal.

DISCUSSION

The SARS-CoV-2 coronavirus causes the COVID-19 disease and its pandemic began in Wuhan in 2019, from where it quickly spread to all of China, Asia and then the rest of the world, which undoubtedly became a huge epidemiological problem and created a serious threat to the broadly understood community [1, 2]. The virus is transmitted mainly by airborne droplets, causing severe pneumonia in some patients with a spectrum of symptoms typical of acute respiratory distress syndrome (ARDS), but with a postulated new and unusual pathophysiology [3]. The infection occurs through direct contact, droplet route and the fecal-oral route [4].

For doctors and scientists, the topic of SARS-CoV-2 coronavirus infections in children is still complex and not fully understood. Serious cases of COVID-19 disease in children are rare but nevertheless are associated with long-term consequences, including neurological, cardiac and pulmonary complications [5]. Until recently, it was considered that the disease rarely affects newborns and is mild in the paediatric population. The clinical features of SARS-CoV-2 coronavirus infection in neonates are mostly non-specific. The most common symptoms occur in the form of respiratory failure, temperature instability. Cardiovascular and digestive system dysfunctions occur primarily in the group of preterm infants [6]. In the group of newborns of mothers with COVID-19 disease, transient tachypnea of newborns, polymorphic rash, prolonged acrocyanosis and adaptation disorders were observed. Acute ME was not considered a common presentation of COVID-19 in paediatrics and the first reports concerned adult patients. However, over time, several paediatric patients with ME associated with SARS-CoV-2 coronavirus infection have been described. The biochemical characteristics of CSF in ME associated with SARS-CoV-2 coronavirus infection include high protein concentration and low pleocytosis <500 cells/μL; the clinical symptoms include fever, vomiting, loose stools, cough without respiratory distress, convex front fontanel, stiff neck, and excessive irritability. Additionally, convulsions are a relatively common symptom of ME in newborns and children, and among the complications, postinflammatory hydrocephalus is quite common [7].

It should be emphasized that data on the risk, route of infection, pathogenesis, clinical symptoms, treatment and prognosis of COVID-19 disease in children, are limited and inconsistent. The transmission of the SARS-CoV-2 coronavirus from an infected pregnant woman to the foetus remains unclear and requires further research. Viraemia in pregnant women occurs in only 1% of cases of COVID-19 disease; therefore, transmission of the virus to the foetus via the placenta in the absence of maternal viremia appears to be a rare phenomenon [8]. This is confirmed by the negative results of RT-PCR tests in the newborns of mothers diagnosed with COVID-19 disease in the perinatal period. The genetic material of the SARS-CoV-2 coronavirus was also not detected in the amniotic fluid and placenta by RT-PCR method [9]. In the presence of viraemia in a pregnant woman, the risk of viral transmission via the placenta to the foetus may be higher [10]. Hence, the droplet route remains the primary route of viral transmission from mother to newborn. In the discussed clinical case, the newborn was most likely infected by airborne droplets from the mother who developed clinical symptoms of COVID-19 disease on the 4th postpartum day. After birth, the newborn remained with the mother in the rooming-in system, but was not breastfed in accordance with the mother's decision; the risk of infection of the newborn by this route was therefore impossible in this case, despite the fact that the genetic material of the SARS-CoV-2 coronavirus is detected in breast milk in approximately 2% of mothers with confirmed SARS-CoV-2 coronavirus infection in the perinatal period [11].

The newborn developed symptoms of severe systemic SARS-CoV-2 coronavirus infection, which was joined by a bacterial infection with microbiologically confirmed bacteraemia. In the course of the infection, the newborn also developed symptoms of viral ME, which was confirmed by a positive result of a general CSF test with lymphocyte-predominant pleocytosis. The results of CSF microbiological tests, including the evaluation of the direct preparation and culture on aerobic media, cannot be considered fully reliable because the patient was treated with antibiotics before the collection of biological material, and in such cases the sensitivity of the CSF microbiological test decreases significantly [12, 13].

The results of CSF tests using the RT-PCR method for the presence of genetic material of aerobic and enveloped bacteria also turned out to be negative, which additionally indicated the viral etiology of ME. A negative result of CSF testing for SARS-CoV-2 coronavirus infection using the RT-PCR method is a quite typical phenomenon, because the current studies have not clearly confirmed the presence of viral genetic material in CSF, except for 1 case in 2020 in Japan. Neurological disorders of both peripheral and central origin

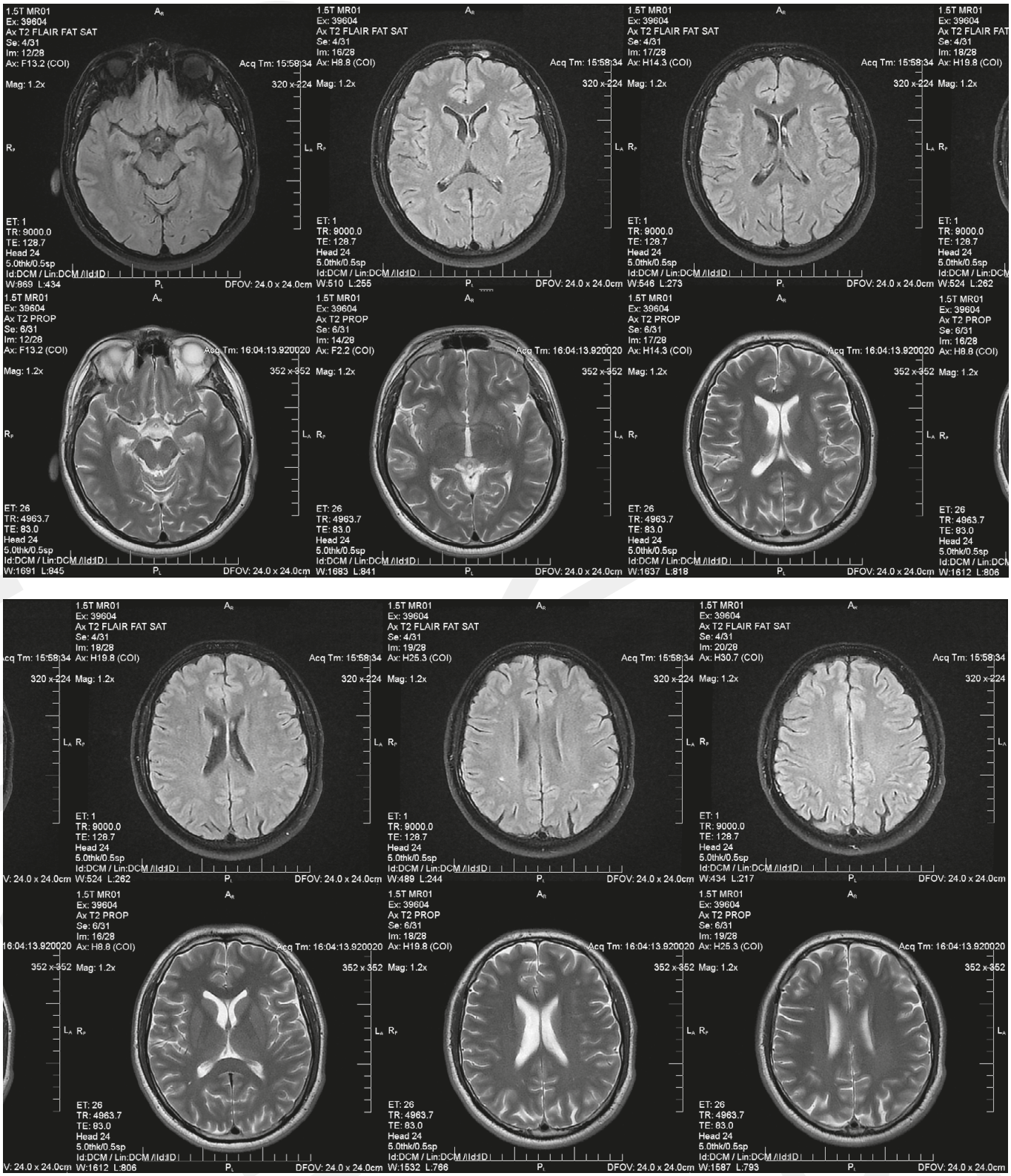

Figure 6. Magnetic resonance imaging of central nervous system. The test was performed on day 71 of life with the GE Optima MR450 1.5T apparatus. The PROPELLER, FLAIR FAT-SAT, DWI, SWAN sequences were used to obtain T1-dependent and T2-dependent images. In the thin film sections made, the presence of areas with increased IS subcortical in the right frontal lobe, visible only in AX FLAIR MPR sections, most likely with the features of the cortical system, draws attention. On both sides, in the frontal parietal area, non-specific foci with elevated IS are visible, most likely corresponding to post-inflammatory changes. In addition, brain tissues with correct signal intensity distribution without focal changes. Symmetrical corpus callosum with correct signal morphology. Lateral ventricles of the brain not displaced, slightly dilated. Evans index – 0.31. Slightly wider space of the arachnoid in the area of the Turkish saddle. No obvious symptoms of increased intracranial pressure. MR image – morphology of the meningeal signal is within normal limits. Cross-sections – pituitary gland not enlarged, no obvious focal changes. No signs of fresh or previous haemorrhage into the structures of the central nervous system

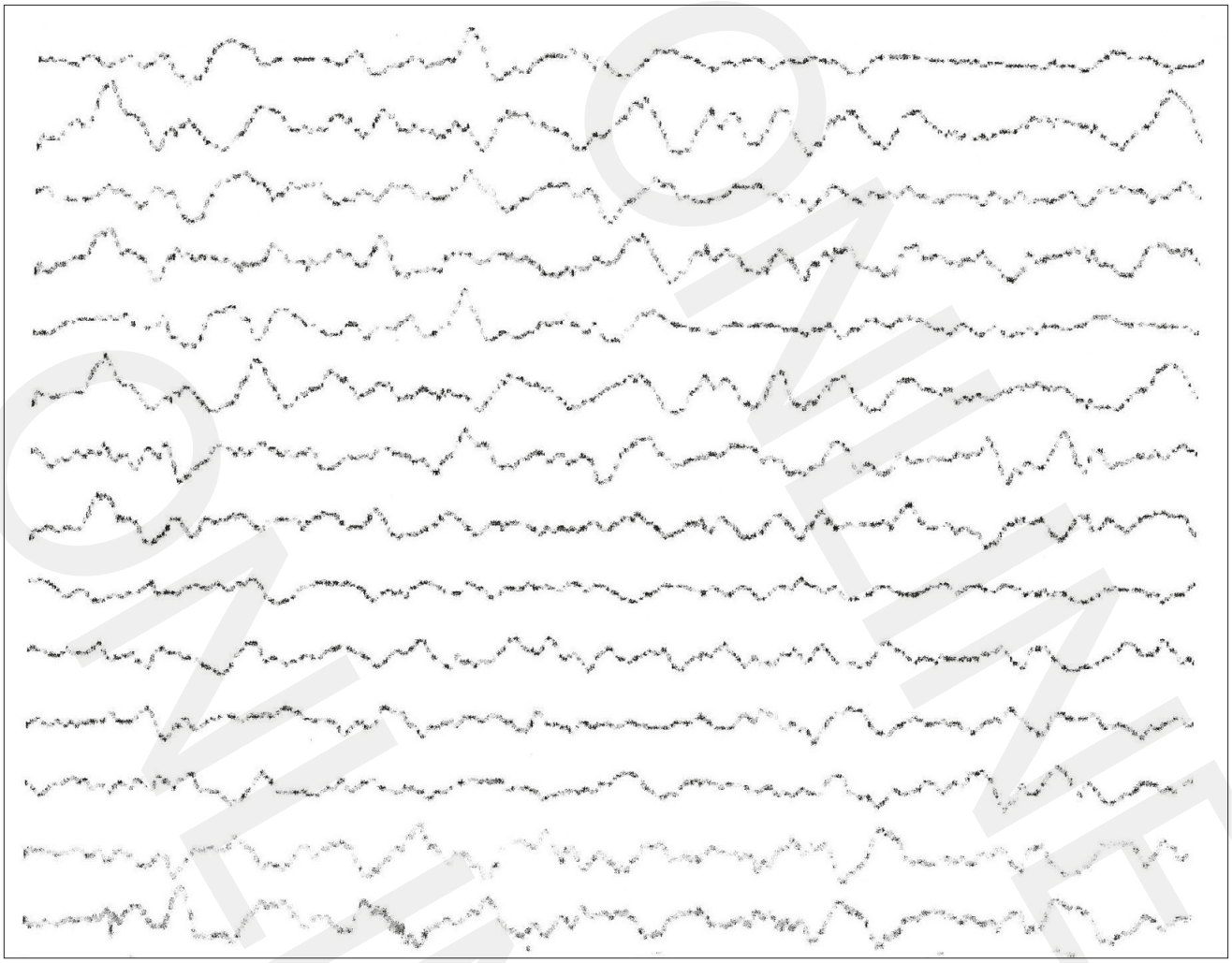

Figure 7. Electroencephalogram (EEG) of the newborn – normal recording. The test was performed during natural sleep. The record of longitudinal and transverse leads was assessed. Normal EEG recording consists of the alpha rhythm, occurring mainly in the parietal and occipital lobe, and the beta rhythm, occurring mainly in the frontal and temporal lobe. Travel speed – 30 mm/s. High frequency filter – 70 Hz. Low frequency filter – 1 Hz. Notch filter – 50 Hz

related to SARS-CoV-2 coronavirus infection is most likely the result of endothelial inflammation, a cytokine storm and activation of immune cells [14, 15].

Despite the negative results of the CSF bacteriological tests, severe clinical condition and staphylococcal bacteraemia, statistically associated with a 10% – 30% risk of ME coexistence, necessitated the use of dual pharmacotherapy in this patient using both antiviral drugs and broad-spectrum antibiotics [16]. The treatment used was VAN – an antistaphylococcal glycopeptide antibiotic, MP – an antibiotic from the group of carbapenems, and CTX – characterized by excellent penetration through the inflamed blood-brain barrier [17, 18, 19]. Molecular virological diagnostics did not show the presence of genetic material of CMV and SARS-CoV-2 coronavirus in CSF. However, due to the results of biochemical examination of the CSF, indicating a viral etiology of ME, ACV was empirically included in the treatment because of the CNS infection caused by other viruses, such as viruses from the Flaviviridae and Enteroviridae families, which could not be clearly excluded [20, 21].

As a pathogenetic factor of the observed hydrocephalus, inflammation should be indicated because it is the most important pathogenetic process in both post-haemorrhagic and post-infectious hydrocephalus. Recent data on the pathogenesis of post-inflammatory hydrocephalus highlight the role of cytokines regulated by signaling pathways, immune cells and the Toll-4 receptor, an endothelial immune receptor that interacts with agonists from both microbes and host cells to stimulate the expression of adhesion particles and chemokines, thus increasing the binding of neutrophils to the endothelium and enhancing leukocyte diapedesis [22, 23].

The increased activity of CA, stimulated by proinflammatory cytokines and immune cells, plays a remarkable role in the pathogenesis of hydrocephalus, and the inhibition of its activity by ACZ independent of the presence of both endogenous and exogenous proinflammatory factors, may play an important therapeutic role. In the discussed case, adding ACZ to the treatment allowed observation of the stabilization and then regression of hydrocephalus, with normalization of the Evans index and reduction of frequency of seizures until their complete resolution. EEG showed no waves typical for epileptic foci, and MRI of the head showed no serious consequences of neuroinfection. The psychophysical development of a child, assessed at 6th months of age, showed it to be proceeding correctly.

In a previous hospital, there were some issues regarding the handling of a newborn during hospitalization that were

not clarified in the documentation provided when the patient was transferred to the NICU that specializes in treating COVID-19 in newborns. Additionally, it was difficult to make unequivocal conclusions about the action of ACZ in the presented clinical case, because the regression of hydrocephalus observed in the patient may have been the result of a complex therapeutic process and the additive and synergistic effect of the combined treatment. This is undoubtedly a limitation of the data obtained. Nevertheless, it is worth noting that despite the correct use of the other drugs administered, including potent anticonvulsants, the patient continued to experience seizures and progressive hydrocephalus. There was a clear clinical improvement only when ACZ was included in the treatment. In the course of its further use, a regression of hydrocephalus was observed with a final reduction of the Evans index from 0.38 to 0.31. The pharmacological action of ACZ to reduce the production of CSF and the reduction of pathological bioelectrical discharges in neurons has been known for years. The data presented in the presented case study seem to confirm this effect, and additionally indicate that the drug may also work in the case of ME and postinflammatory hydrocephalus in the course of COVID-19 disease, especially because popular antiviral drugs used in the treatment of COVID-19 disease, such as molnupiravir and Remdesivir are not approved for neonatal treatment. There is insufficient evidence that they achieve therapeutic concentrations in CNS tissues, and have no hard indications for the treatment of neurological and psychiatric complications in SARS-CoV-2 infection [24, 25, 26, 27]. The use of ACZ may limit the dynamics of hydrocephalus growth which, in turn, may reduce the frequency of neurosurgical interventions that are at risk of complications, especially in the presence of acute CNS infections. In order to clearly answer the question to what extent ACZ affects the dynamics of hydrocephalus, a wide clinical trial should be conducted in patients with ME, seizures and hydrocephalus of SARS-CoV-2 etiology, and a control group with similar disease entities but of a different etiology.

REFERENCES

1. Li Q, Guan X, Wu P, et al. Early transmission dynamics in Wuhan, China, of novel coronavirus-infected pneumonia. N Engl J Med. 2020;382(13):1199–1207. http://doi.org/10.1056/NEJMoa2001316
2. Xu B, Gutierrez B, Mekaru S, et al. Epidemiological data from the COVID-19 outbreak, real-time case information. Sci Data. 2020;7(1):106. http://doi.org/10.1038/s41597-020-0448-0
3. Navas-Blanco JR, Dudaryk R. Management of respiratory distress syndrome due to COVID-19 infection. BMC Anesthesiol. 2020;20(1):177. http://doi.org/10.1186/s12871-020-01095-7
4. Delikhoon M, Guzman MI, Nabizadeh R, et al. Modes of transmission of severe acute respiratory syndrome-coronavirus-2 (SARS-CoV-2) and factors influencing on the airborne transmission: a review. Int J Environ Res Public Health. 2021;18(2):395. https://doi.org/10.3390/ijerph18020395
5. Nalbandian A, Sehgal K, Gupta A, et al. Post-acute COVID-19 syndrome. Nat Med. 2021;27:601–615. http://doi.org/10.1038/s41591-021-01283-z
6. Kumar VHS, Prasath A, et al. Respiratory failure in an extremely premature neonate with COVID-19. Children (Basel). 2021;8(6):477. http://doi.org/10.3390/children8060477
7. Arango Ferreira C, Correa-Roda M. Acute meningoencephalitis as initial presentation of SARS-CoV-2 infection in pediatrics. Pediatr Infect Dis J. 2020;39(11):e386-e387. https://doi.org/10.1097/INF.0000000000002885
8. Wang W, Xu Y, Gao R, et al. Detection of SARS-CoV-2 in different types of clinical specimens. JAMA. 2020;323(18):1843–1844. http://doi.org/10.1001/jama.2020.3786
9. Chen H, Guo J, Wang C, et al. Clinical characteristics and intrauterine vertical transmission potential of COVID-19 infection in nine pregnant women: a retrospective review of medical records. Lancet. 2020;395(10226):809–815. https://doi.org/10.1016/S0140-6736(20)30360-3
10. Chen W, Lan Y, Yuan X, et al. Detectable 2019-nCoV viral RNA in blood is a strong indicator for the further clinical severity. Emerg Microbes Infect. 2020;9(1):469–473. https://doi.org/10.1080/22221751.2020.1732837
11. Kumar J, Meena J, Yadav A, et al. SARS-CoV-2 detection in human milk: a systematic review. J Matern Fetal Neonatal Med. 2021:1–8. http://doi.org/10.1080/14767058.2021.1882984
12. Wagner K, Springer B, Pires VP, et al. Pathogen identification by multiplex lightmix real-time PCR assay in patients with meningitis and culture-negative cerebrospinal fluid specimens. J Clin Microbiol. 2018;56(2):e01492–17. https://doi.org/10.1128/JCM.01492-17
13. Rogers T, Sok K, Erickson T, et al. Impact of antibiotic therapy in the microbiological yield of healthcare-associated ventriculitis and meningitis. Open Forum Infect Dis. 2019;6(3):ofz050. http://doi.org/10.1093/ofid/ofz050
14. Bellon M, Schweblin C, Lambeng N, et al. Cerebrospinal fluid features in severe acute respiratory syndrome coronavirus 2 (SARS-CoV-2) reverse transcription polymerase chain reaction (RT-PCR) positive patients. Clin Infect Dis. 2021;73(9):e3102-e3105. https://doi.org/10.1093/cid/ciaa1165.\
15. Abdel-Mannan O, Eyre M, Löbel U, et al. Neurologic and radiographic findings associated withhttp://doi.org/10.1186/s13052-018-0573-y COVID-19 infection in children. JAMA Neurol. 2020;77(11):1440–1445. https://doi.org/10.1001/jamaneurol.2020.2687
16. May M, Daley AJ, Donath S, et al. Australasian study group for neonatal infections. Early onset neonatal meningitis in Australia and New Zealand, 1992–2002. Arch Dis Child Fetal Neonatal Ed. 2005;90:F324-F327. http://doi.org/10.1136/adc.2004.066134
17. Salmon-Rousseau A, Martins C, Blot M, et al. Comparative review of imipenem/cilastatin versus meropenem. Med Mal Infect. 2020;50(4):316–322. https://doi.org/10.1016/j.medmal.2020.01.001
18. Bryce AN, Doocey R, Handy R. Staphylococcus haemolyticus meningitis and bacteremia in an allogenic stem cell transplant patient. IDCases. 2021;26:e01259. https://doi.org/10.1016/j.idcr.2021.e01259
19. Chen XK, Shi HY, Leroux S, et al. Penetration of cefotaxime into cerebrospinal fluid in neonates and young infants. Antimicrob Agents Chemother. 2018;62(4):e02448–17. https://doi.org/10.1128/AAC.02448-17
20. O'Leary CK, Jones C, Bryant PA, et al. Feasibility of continuous Infusions of acyclovir. Pediatr Infect Dis J. 2020;39(9):830–832. https://doi.org/10.1097/INF.0000000000002692
21. Schaenman JMD, Ho Dy, Baden LR, et al. Enterovirus infection in immunocompromised hosts. In: Safdar A, editors. Principles and practice of transplant infectious diseases. New York, NY: Springer. https://doi.org/10.1007/978-1-4939-9034-4_42
22. Chen F, Zou L, Williams B, et al. Targeting toll-like receptors in sepsis: from bench to clinical trials. Antioxid Redox Signal. 2021;35(15):1324–1339. https://doi.org/10.1089/ars.2021.0005
23. Ma X, Tian D, Lv W, et al. Anti-inflammatory effects of microRNA-223 on sepsis-induced lung injury in rats by targeting the Toll-like receptor signaling pathway. Exp Ther Med. 2021;22(3):964. http://doi.org/10.3892/etm.2021.10396
24. Saravolatz LD, Depcinski S, Sharma M. Molnupiravir and nirmatrelvir-ritonavir: oral COVID antiviral drugs. Clin Infect Dis. 2022: ciac180. http://doi.org/10.1093/cid/ciac180
25. Painter GR, Natchus MG, Cohen O, et al. Developing a direct acting, orally available antiviral agent in a pandemic: the evolution of molnupiravir as a potential treatment for COVID-19. Curr Opin Virol. 2021;50:17–22. http://doi.org/10.1016/j.coviro.2021.06.003
26. García CAC, Sánchez EBA, Huerta DH, et al. Covid-19 treatment-induced neuropsychiatric adverse effects. Gen Hosp Psychiatry. 2020;67:163–164. http://doi.org/10.1016/j.genhosppsych.2020.06.001
27. Yang K. What do we know about remdesivir drug interactions? Clin Transl Sci. 2020;13(5):842–844. http://doi.org/10.1111/cts.12815